A. Benninghoven, P. Bertrand, H.-N. Migeon and H.W. Werner (Editors).
Proceedings of the 12th International Conference on Secondary Ion Mass Spectrometry,
Brussels, Belgium, 5-11 September 1999

HOW DO LARGE ORGANIC MOLECULES SPUTTER ? INSIGHTS FROM TOF-SIMS AND MOLECULAR DYNAMICS SIMULATIONS.

A. Delcorte,[1+] P. Bertrand,[2] J. C. Vickerman[3] and B. J. Garrison[1]

[1]Department of Chemistry, The Pennsylvania State University, 152 Davey Lab, University Park, PA 16802,USA

[2]PCPM, Universite catholique de Louvain, 1 Croix du Sud, B1348, Louvain-la-Neuve, Belgium

[3]Surface Analysis Research Centre, Department of Chemistry, UMIST, PO Box 88, Manchester, M60 1QD, UK

[+]phone: 1-(814)-863-2108; fax: 1-(814)-863-5319; e-mail: delcorte@chem.psu.edu

1. Introduction

The bombardment of organic solids by keV ions induces the emission of molecular species, including characteristic fragments and large parent-like ions, which form the useful secondary ion signal. Unfortunately, it also produces small, uncharacteristic or considerably rearranged fragments, constituting an additional 'noise' that gives rise to amazingly complex spectra. Although several important advances arise from empiricism (heavy metal substrates, ionic salt matrices or polyatomic projectiles), as scientists, we would like to base future improvements on a fundamental understanding of the molecular ion emission mechanisms. From an experimental study based on the interpretation of kinetic energy distributions (KED) of molecular ions, new insight was gained into the energy transfer process and reaction channels involved in the formation of the observed ejected species [1]. To complement this work, molecular dynamics simulations have been initiated recently, with polystyrene (PS) tetramers and dibenzanthracene (DBA) molecules adsorbed on Ag{111} as the model systems for the investigation of the mechanisms of polyatomic fragment ejection. In this review, the good match often found between simulation and experiment will be highlighted, as well as the results that are more challenging to model.

2. Methods

2.1. ToF-SIMS experiments. Thin organic layers were formed by solution casting onto a clean polycrystalline silver support [2]. The organic molecules were sec-butyl ended polystyrene tetramers ($C_4H_9(C_8H_8)_4H$) and dibenzanthracene ($C_{22}H_{14}$). The samples were bombarded with a (5 kHz) pulsed Ga^+ beam (15 keV) and the secondary ions were mass- and energy- analyzed in a Phi-Evans TRIFT1 Time-of-Flight SIMS [3]. The angle between the ion gun and the normal to the sample surface was 35°. In this system, the accelerated secondary ions are energy-selected by an energy slit (1.5 eV passband) inserted at the crossover following the first hemispherical electrostatic analyzer. The detailed procedure to measure KEDs has been described in Ref. [4].

2.2. MD simulations. In the model, the silver substrate is approximated by a finite microcrystallite containing 1404 Ag atoms arranged in 9 layers of 156 atoms each. Either five

PS tetramers or six DBA molecules were placed on the Ag surface. Ar atoms (500 eV) were directed parallel to the surface normal. Four thousand trajectories were calculated for the PS/Ag system, and one thousand trajectories with the DBA/Ag system. A fresh undamaged sample was used for each trajectory. The integration scheme as well as the many-body and pairwise potentials used in the simulation have been described elsewhere [5]. The hydrocarbon interactions were described by the Brenner hydrocarbon potential function [6,7] thus allowing us to model chemical reactions.

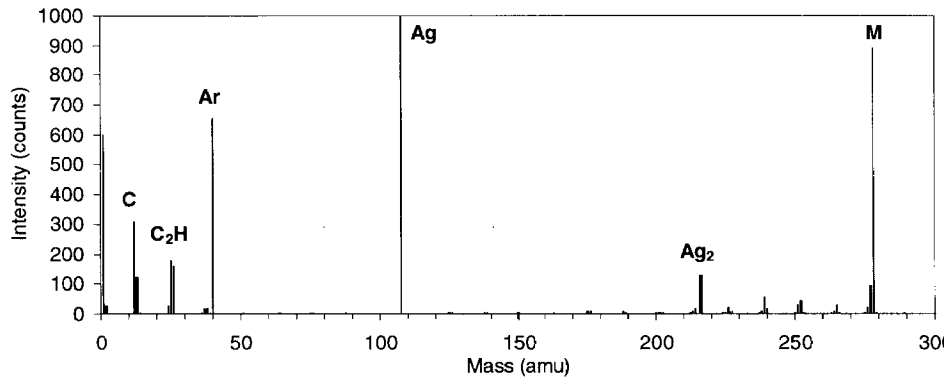

Fig. 1. Calculated neutral mass spectrum obtained after the bombardment of DBA/Ag{111} by 500 eV Ar atoms at 6 ps.

3. Experimental and calculated mass spectra

In SIMS analysis, the information is typically provided by the mass spectrum. It is the result of the combined action of several processes, including collision cascades, fragmentation in the surface region, ionization and metastable decay in the vacuum. Obviously, current MD simulations cannot account for ionization processes and long-lifetime metastable decay. Nevertheless, it will be shown in the following discussion that the comparison between the results from experiment and simulation yields insight into these processes also. In particular, the similarities and differences between the calculated and experimental mass spectra may be used as a key to start the analysis of the emission mechanisms in SIMS. The calculated mass spectrum of DBA on silver is shown in Fig. 1. The main peaks in the low-mass region (below 100 amu) correspond to small hydrocarbon fragments with one to three carbon atoms. In the high-mass region (beyond 100 amu), beside the entire molecule, there is a less intense series of fragments with more than ten carbon atoms. The main hydrocarbons of the high-mass region, including the entire molecule, correspond to the formula C_xH_{x-8}. For comparison purpose, the partial SIMS spectrum of DBA (region between 200 and 300 amu) can be found in Ref. 8. The main peaks are the same C_xH_{x-8} (252, 265, 278 amu), but beside these species, the spectrum also exhibits intense hydrogen-deficient fragments that are not found in the calculated spectrum (250, 263, 276 amu). The calculated spectrum of DBA will serve as an example to guide us into the fundamentals of the emission mechanisms.

4. Kinetic energy distributions: a means to elucidate fragmentation and metastable decay processes

A striking difference between the high-mass range of the DBA spectra is the quasi-absence of $C_{22}H_{12}$ in the simulation versus its high intensity in the experiment. To understand this difference, it is helpful to look at the experimental KED of $C_{22}H_{12}^+$ (Fig. 2). Beside the narrow peak in the positive range of the KED (peak I), a large fraction of the intensity is observed at 'negative energies' (peaks II and III). The two peaks and their oblique baseline correspond to $C_{22}H_{12}^+$ with a significant energy deficit with respect to the full acceleration energy. In fact, all these ions have been formed by metastable decay of larger parent ions either in the acceleration or in the field-free drift section of the spectrometer, transferring a part of their energy to the undetected neutral product [8]. Peak III corresponds to H_2 loss from $C_{22}H_{14}^+$, peak II to a single H loss from $C_{22}H_{13}^+$, and the baseline to unidentified reactions in the acceleration section. For this ion, the overall intensity fraction corresponding to metastable reactions occurring *after* 10^{-9} s is more than 75 % of the total intensity. Unimolecular dissociation happening *before* 10^{-9} s will lead to energies included in peak I and, therefore, cannot be distinguished from direct emission of the fragment. Thus, Fig. 2 shows that the major part of the peak $C_{22}H_{12}^+$ in the experimental spectrum of DBA is due to late metastable decay reactions in the vacuum. This is also true for most of the other hydrogen-deficient fragments observed in the spectrum of DBA and for the polycyclic aromatic ions in the spectrum of PS [8].

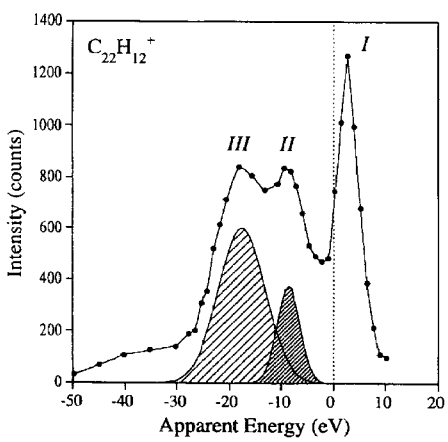

Fig. 2. Kinetic energy distribution of $C_{22}H_{12}^+$ (276 amu) sputtered from DBA on Ag. The Gaussian curves (hatched areas) indicate the calculated area of the identified H (II) and H_2 loss peaks (III). From Ref. [8].

Such late metastable decay events will not be observed in MD simulations where the timescale is limited to a few picoseconds. Moreover, it is not clear whether the Brenner hydrocarbon potential is appropriate to model elimination reactions such as H_2 loss. Nevertheless, the metastable decay rate depends directly on the internal energy of the fragments, which is accessible from MD. Thus, it is possible to define an internal energy threshold beyond which the sputtered particle will not be stable enough to be detected and to filter the 'stable' fragments in the MD results. Examples of adequate internal energy

thresholds can be found in the literature. For instance, the naphthalene and phenanthrene cations will not be detected if they have more than 7 and 7.5 eV of internal energy, respectively [9]. The mass spectra and other properties like the KEDs and the angular distributions can be corrected using this internal energy threshold [5]. To illustrate this feature, PS is more appropriate as an example than DBA because it produces a whole range of characteristic fragments with a significant intensity between 0 and 100 amu. In Fig. 3a, the correction has been implemented for two characteristic fragments of PS with markedly different sizes, C_2H_2 and C_7H_7, using a 7.5 eV threshold for both species. The calculated KEDs were also corrected to mirror the 2 eV energy resolution of the experiment. The high energy tail of the KED of C_7H_7 (dots) is depleted when excited particles are excluded (dashed line), and the agreement with the experimental KED (Fig. 3b) becomes much better. Fig. 3 compares the experimental KED of $C_2H_3^+$ to the calculated KED of C_2H_2. Indeed, the intensity of C_2H_3 is weak in the simulation and the KED of the intense C_2H_2 averages the noisy distribution of C_2H_3. In contrast with C_7H_7, the KED of C_2H_2 does not change after correction, and remains very similar to the experimental KED of $C_2H_3^+$.

Fig. 3. Kinetic energy distributions of fragments sputtered from PS oligomers. (a) Simulation: C_7H_7 with (---) and without (•••) a 7.5 eV internal energy filter. (b) Experiment (2 eV passband).

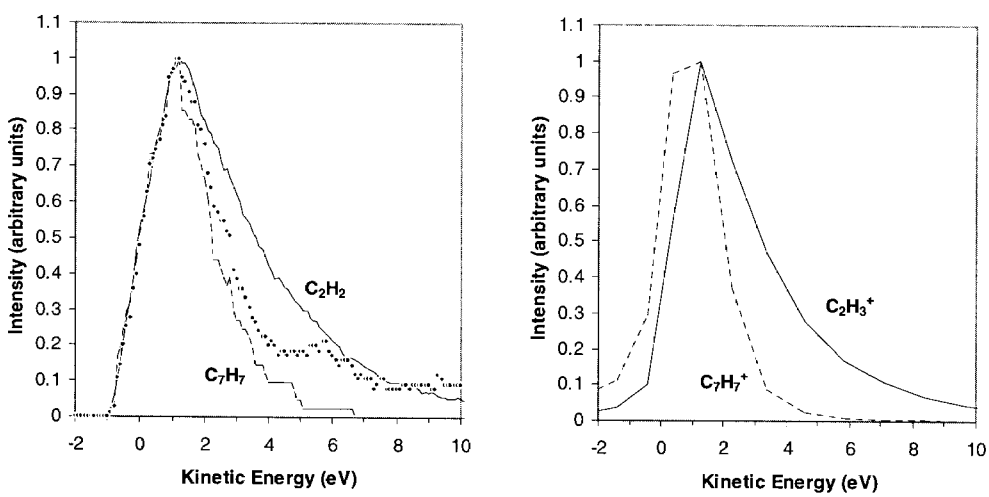

From the point of view of the emission mechanisms, the results of Fig. 3 are important because they show that characteristic fragments of PS like C_7H_7 can be sputtered by collisional mechanisms. In addition, the reduction of the mean kinetic energy with increasing fragment size [1] can be explained partly by the nature of the collisional interaction (non-corrected distribution of C_7H_7 versus C_2H_2) and partly by the internal energy-dependent dissociation of excited fragments (corrected distribution of C_7H_7). On the other hand, the fact that the experimental KED of $C_7H_7^+$ is shifted towards negative energies suggests that a

significant fraction of the 'positive energy' peak of $C_7H_7^+$ can be attributed to unimolecular dissociation, too (Fig. 3b).

In the experiments, the average kinetic energy of DBA parent ions and Ag-cationized PS oligomers is unexpectedly high, as indicated by the width and high-energy tail of the KEDs [2]. Although the uncorrected KEDs calculated by MD are close to that obtained in the experiment, the internal-energy filtered KEDs of entire molecules are significantly thinner when a 7.5 eV stability threshold is used. To explain this disagreement, we propose that the value of the stability threshold might significantly depend on the fragment size. The implementation of a more realistic, size-dependent stability threshold based on the RRK theory is one of our major priorities.

5. Emission mechanisms as revealed by the MD simulation

To understand the emission mechanisms of fragments and parent molecules, a representative set of trajectories has been analyzed in detail. A major ejection scenario emerges from the MD simulation to explain the ejection of molecular fragments from flat molecules like DBA and PS tetramers (as opposed to vertical alkyl [10] and alkanethiol chains [11]). It appears indeed that the early and direct collision between the primary particle and a carbon atom of the molecule is the most efficient way to produce fragments. For PS tetramers, the implantation of one backbone atom in the substrate, followed by a second bond-breaking due to another moving carbon atom (or a small hydrocarbon) resulting from the primary particle impact, is an efficient way to release characteristic fragments with a low internal energy from inside the chain. This mechanism will be described at length in Ref.12. Instead, collision cascades developing in the silver substrate mainly lead to the ejection of entire molecules.

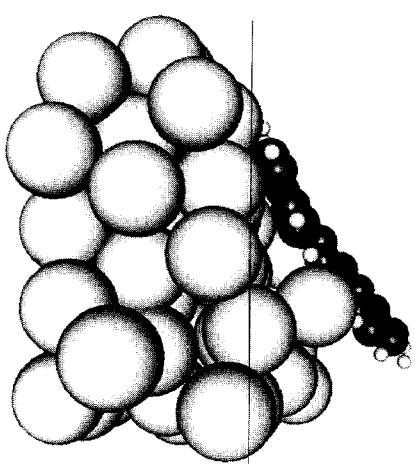

Fig. 4. Side view of an event showing the uplifting of a DBA molecule by several silver atoms. Silver is light grey and carbon is dark grey. The plane of the original silver surface, perpendicular to the page, is indicated by the full line. The molecule is pushed upwards by three silver atoms.

For entire PS and DBA molecules, MD simulations indicate two possible emission scenarios. First, the ejection can be induced by a single, energetic silver atom. Second, the

molecule liftoff may be the result of the interaction with two, or more, moving silver atoms (cooperative uplifting). The first scenario is likely to produce molecules with a large amount of vibrational motion, as well as the interaction with several silver atoms having completely uncorrelated velocity vectors. For the flexible PS tetramers (and to a lesser extent for the stiff and lighter DBA molecules), the uplifting by several substrate atoms with quite similar velocity vectors will be the most efficient way to desorb 'cool' molecules with the high kinetic energy indicated by the experiments. This 'soft' uplifting mechanism is illustrated in Fig. 4 for DBA.

6. Conclusion

The combined approach including experimental measurements and MD simulations appears promising to elucidate the emission and fragmentation of organic molecules in SIMS. The MD simulation allows us to isolate collisionally-induced processes, excluding electronic and ionization effects as well as late metastable decay mechanisms. The influence of late metastable decay may be estimated using an internal energy filter for the sputtered fragments. As the introduction of ionization mechanisms in the MD code is not straightforward, the easiest way to overcome this limitation would be to postionize neutral fragments and molecules in the experiment. Concerning mechanisms, the detailed analysis of calculated trajectories showed that the direct interaction with the primary particle is very efficient to generate characteristic fragments, whereas collision cascades tend to eject entire molecules. The ejection of stable PS tetramers with more than 1-2 eV of kinetic energy and, furthermore, of larger organic molecules, is most likely to occur via a soft uplifting mechanism induced by several substrate atoms with similar momenta.

Acknowledgements. The authors (AD and BJG) would like to acknowledge the support from the National Science Foundation. Additional computational resources were provided by the Center for Academic Computing. AD and PB are grateful to the *Communaute Francaise de Belgique* which supported this work through its *Action de Recherche Concertee* (94/99-173). The ToF-SIMS equipment was acquired with the support of the *Region Wallonne* and *FRFC-Loterie Nationale* of Belgium.

References

[1] P.Bertrand and A.Delcorte, SIMS XI Proceedings; G.Gillen, R.Lareau, J.Bennett and F.Stevie (Eds.), Wiley, New York, (1998), p 437, and references therein.
[2] A.Delcorte and P.Bertrand, Surf.Sci.J. 412/413 (1998) 97-124.
[3] B.W.Schueler, Microsc.Microanal.Microstruct. 3 (1992) 119.
[4] A.Delcorte and P.Bertrand,.Nucl. Instr. And Meth. B 115 (1996) 246.
[5] R.Chatterjee, Z.Postawa, N.Winograd, B.J.Garrison, J. Phys. Chem. B 103 (1999) 151.
[6] D.W.Brenner, Phys.Rev. B 42 (1990) 9458.
[7] W.Brenner, J.A.Harrison, C.T.White, R.J.Colton, Thin Solid Films 206 (1991) 220.
[8] A.Delcorte, B.G.Segda and P.Bertrand, Surf.Sci.381 (1997) 18.
[9] Y.Gotkis, M.Oleinikova, M.Naor and C.Lifshitz, J. Phys. Chem. 97 (1993) 12282.
[10] R.S.Taylor and B.J.Garrison, Langmuir 11 (1995) 1220.
[11] K.S.S.Liu, C.W.Yong, B.J.Garrison, J.C.Vickerman, J. Phys. Chem. B 103 (1999) 3195.
[12] A.Delcorte, X.Vanden Eynde, P.Bertrand, J.C.Vickerman, B.J.Garrison, unpublished.